

Uniting Low- and High-Sensitivity Experiments through Generalised NMR Supersequences

Jonathan R. J. Yong,¹ Ēriks Kupče,² Tim D. W. Claridge^{1,*}

¹ *Chemistry Research Laboratory, Department of Chemistry, University of Oxford, Mansfield Road, Oxford, OX1 3TA, United Kingdom*

² *Bruker UK Ltd, R&D, Coventry CV4 9GH, United Kingdom*

* tim.claridge@chem.ox.ac.uk

<https://www.rsc.org/journals-books-databases/about-journals/chemcomm#writing-guidelines>

<https://www.rsc.org/journals-books-databases/author-and-reviewer-hub/authors-information/prepare-and-format/>

TODO: TOC graphic and TOC text (15–25 words)

In terms of length, the main text (without figures or references) forms approximately 2.5 pages when transferred to the RSC template.

Abstract

NOAH supersequences represent a time-efficient way of collecting multiple 2D NMR experiments. We show here that experiments with very different sensitivity requirements, including 1,1-ADEQUATE and HSQC, may be efficiently combined through interleaved supersequences which effectively assign each module a different number of transients. Such sequences fully generalise the concept of ‘parallel’ supersequences, abolishing all remaining restrictions on the number of spectra acquired in a single experiment.

(66 words; the template suggests 50 words...)

1 Introduction

Nuclear magnetic resonance (NMR) spectroscopy plays a key role in the structural elucidation of natural products; in particular, two-dimensional (2D) NMR experiments provide vast amounts of information on through-bond and through-space molecular connectivity.^{1,2} However, these experiments are often time-consuming as they require the incrementation of indirect-dimension evolution periods in order to construct the requisite 2D data matrices. One particularly flexible method for accelerating 2D data acquisition is the NOAH (NMR by Ordered Acquisition using ¹H detection) technique,^{3,4} in which multiple 2D experiments (‘modules’) are combined into a single experiment using only a single recovery

delay. These nested ‘supersequences’, which rely on the tailored excitation of magnetisation from different sources, provide an array of 2D spectra (up to 10 so far) in greatly reduced experiment times.

Virtually all common 2D experiments, such as HMBC, HSQC, COSY, TOCSY, and NOESY, have been implemented in NOAH supersequences, allowing for the (computer-assisted) structural elucidation of a wide range of molecules.^{5–7} However, even these may fall short in proton-sparse molecules^{8–10} which do not yield sufficient correlations. In such cases, recourse must be made to other experiments which typically detect either long-range X–¹H couplings (as in the HMBC experiment,^{11,12} X = ¹³C or ¹⁵N), or ¹³C–¹³C correlations (as in the INADEQUATE¹³—or more practically, ADEQUATE^{14,15}—experiments). Although these rely on heteronuclei (or pairs thereof) with low natural abundances, they allow chemists to directly trace out carbon- and nitrogen-containing backbones with much greater certainty. Furthermore, with the introduction of cryogenically cooled probes and concomitant advances in achievable signal-to-noise ratios (SNRs), such experiments can nowadays be feasibly run even on dilute samples.

To date, insensitive experiments such as ¹⁵N HMBC and ADEQUATE have not been the main focus of NOAH supersequences.¹⁶ This is because in a traditional ‘linear’ supersequence, each constituent module is recorded with the same number of transients. The total experiment duration is therefore dictated by the module with the lowest sensitivity, and higher-sensitivity modules (e.g. HSQC or COSY) would be recorded with far more transients than would be necessary. Although the more sensitive modules would still be obtained ‘for free’, the *effective* time savings thus realised would be far smaller than for a supersequence with balanced sensitivities.

For this reason, the low-sensitivity ADEQUATE and ¹⁵N HMBC modules form a ‘natural’ pairing in a NOAH-2 AB_N supersequence (Figure 1b). However, we also go beyond this to add more sensitive modules: not using ‘horizontal’ concatenation as in a traditional supersequence, but instead through ‘vertical’ interleaving, in a similar fashion to the ‘parallel’ supersequences recently described.⁷ This approach, which effectively amounts to tailoring the number of transients for each module, provides a powerful and flexible way to balance modules with different sensitivities. We show that up to four modules (¹⁵N HMBC, ¹³C HMBC, ¹⁵N sensitivity-enhanced HSQC (seHSQC), and ¹³C HSQC) may be interleaved in this fashion (Figures 1d and 1e), thereby fully generalising our previous work on parallel supersequences, which only switched between two modules at a time.

2 NOAH-2 AB_N

When designing NMR supersequences, it is generally a good rule of thumb to place the module with the lowest sensitivity first: this is because any incomplete preservation of magnetisation by earlier modules will lead to decreased sensitivity in later modules. The 1,1-ADEQUATE module, which relies on neighbouring pairs of ¹³C isotopes—occurring only in roughly 1 out of 8130 molecules—therefore forms the beginning of all the supersequences described here.

The ADEQUATE module (Figure 1a) is designed to only use the magnetisation of protons directly bonded to ¹³C, which we denote here as ¹H^C.^{18,19} In order to maintain the sensitivity of later modules, it must return

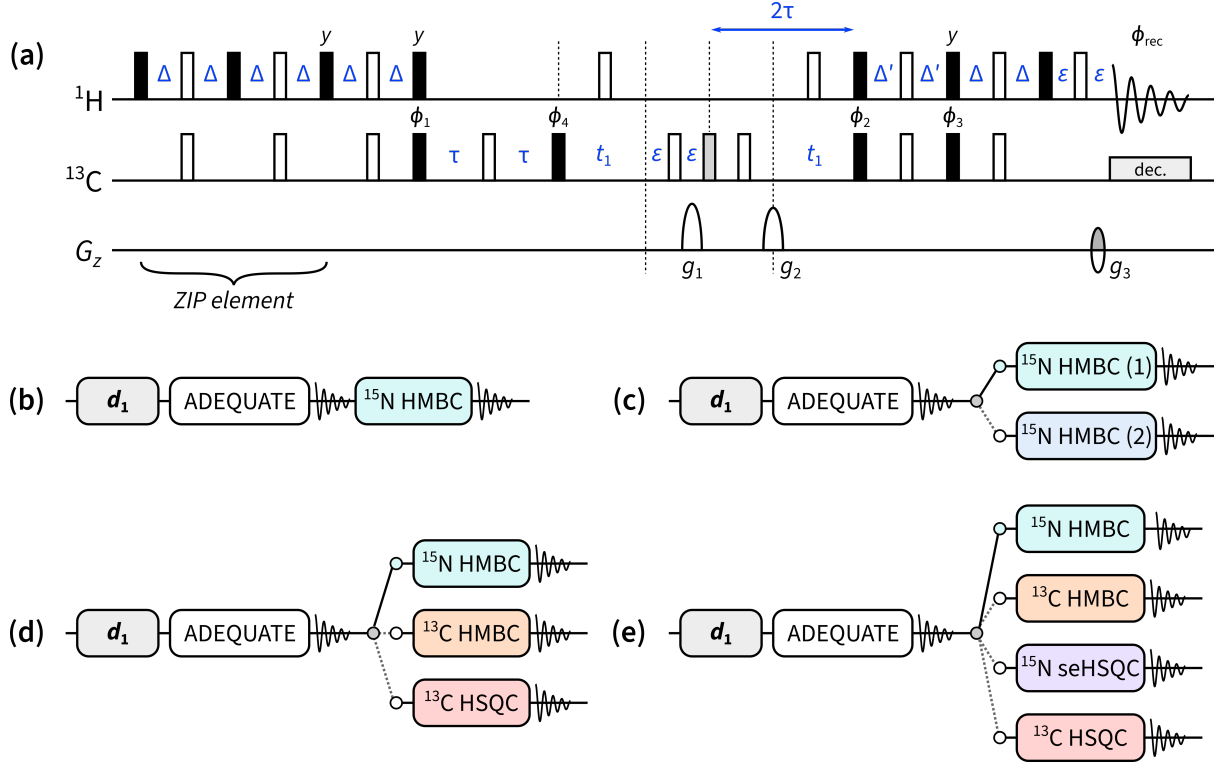


Figure 1: Pulse sequences described in this work. **(a)** ZIP-1,1-ADEQUATE module. Filled and empty bars refer to 90° and 180° pulses respectively; the grey filled bar is a 120° pulse for ^{13}C double-quantum to single-quantum coherence transfer.¹⁷ Pulse and receiver phases are: $\phi_1 = x, -x$; $\phi_2 = 2(x), 2(-x)$; $\phi_3 = 2(y), 2(-y)$; $\phi_4 = 4(x), 4(-x)$; $\phi_{\text{rec}} = x, -x, -x, x, -x, x, x, -x$. Delays are set as follows: $\Delta = 1/(4 \cdot ^1J_{\text{CH}})$, $\Delta' = 1/(8 \cdot ^1J_{\text{CH}})$, and $\tau = 1/(4 \cdot ^1J_{\text{CC}})$. ϵ is the minimum time required for a pulsed field gradient and the following recovery delay. Gradient amplitudes as a percentage of the maximum amplitude (53 G/cm) are: $g_1 = 78.5\%$, $g_2 = 77.6\%$, and $g_3 = -59\%$. Echo-antiecho selection is achieved by inverting the sign of g_3 as well as the pulse phase ϕ_3 . **(b)** NOAH-2 AB_N supersequence. **(c)** NOAH-3 $\text{AB}_\text{N} \text{B}_\text{N}$, where the two ^{15}N HMBC experiments are optimised for two different values of $^nJ_{\text{NH}}$. **(d)** NOAH-4 $\text{AB}_\text{N} \text{BS}$. **(e)** NOAH-5 $\text{AB}_\text{N} \text{BS}_\text{N}^+ \text{S}$.

the magnetisation of all other protons (denoted as $^1\text{H}^{1\text{C}}$) to the equilibrium $+z$ state. This is accomplished by replacing the initial 90° excitation pulse by the zz -isotope selective pulse element (ZIP),^{19,20} which effects 90°_{-x} and 90°_{-y} rotations on $^1\text{H}^\text{C}$ and $^1\text{H}^{1\text{C}}$ magnetisation respectively. (Other isotope-specific elements such as BANGO^{21–23} may also be used here, with similar results generally being obtained.¹⁹) The ^{15}N HMBC module of choice is a simple magnitude-mode version, with an optional first-order low-pass J-filter. In the NOAH-2 AB_N supersequence (ADEQUATE + ^{15}N HMBC, Figure 1b), this module simply consumes the remaining $^1\text{H}^{1\text{C}}$ magnetisation which was preserved by the ZIP-ADEQUATE.

3 NOAH-3 $\text{AB}_\text{N} \text{B}_\text{N}$

Although this sequence on its own performs well (Figure 2), it suffers from the drawback that the ^{15}N HMBC is optimised for one specific value of $^nJ_{\text{NH}}$. In practice, $^nJ_{\text{NH}}$ values range from 2–16 Hz; in a single

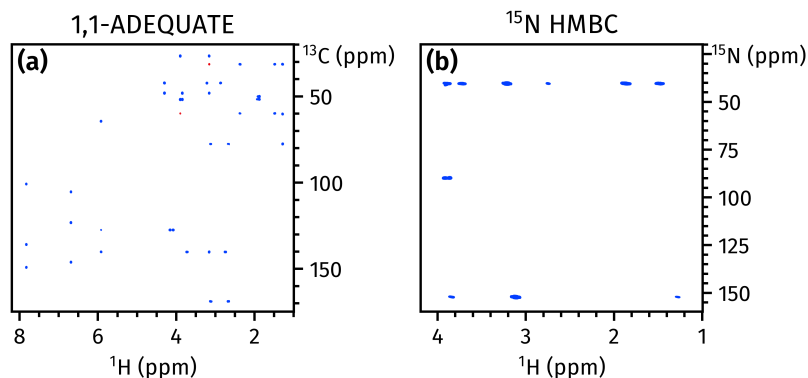


Figure 2: Spectra obtained from the NOAH-2 AB_N supersequence. (a) 1,1-ADEQUATE. (b) ¹⁵N HMBC. Spectra were obtained on a 700 MHz Bruker AV III equipped with a TCI H/C/N cryoprobe; the sample used was 50 mM brucine in CDCl₃.

HMBC experiment, some correlations may therefore be lost due to J-coupling mismatch.

To circumvent this issue, a variety of accordion-type experiments^{24–28} have been designed which decrement the J-evolution period in step with t_1 , allowing a wider range of couplings to be sampled. Here, we adopt the simpler approach of recording two separate HMBC experiments optimised for different $^nJ_{\text{NH}}$ values. This cannot be performed *sequentially* as the two HMBC experiments would draw on the same ¹H¹³C magnetisation, causing the second to suffer from severely decreased sensitivity. However, they can easily be done in an *interleaved* manner where, after the ADEQUATE module, the two HMBC experiments are alternately acquired (Figure 1c).⁷ As the ¹⁵N dimension is typically sparse and a high resolution is not required, we choose to run both ¹⁵N HMBC spectra with half the usual number of t_1 increments compared to the ADEQUATE. As can be seen in Figure 3, the two HMBC spectra reveal different sets of correlations.

4 NOAH-4 AB_NBS

In the above spectra and in previous work,⁷ we have shown how two alternating modules can be used to construct parallel supersequences. Naturally, this concept can be further generalised to use $N \geq 2$ alternating ‘threads’. This is demonstrated using the NOAH-4 AB_NBS supersequence (Figure 1d), in which the ADEQUATE module is followed by either a ¹⁵N HMBC, ¹³C HMBC, or ¹³C HSQC. Because these three latter modules do not have the same intrinsic sensitivity, we balance this by allocating a different number of threads to each module. For example, with $N = 8$, we can acquire the ¹⁵N HMBC six times and the ¹³C HMBC and HSQC once each. After summation of the data, this effectively amounts to acquiring the ADEQUATE experiment with $8n$ transients, the ¹⁵N HMBC with $6n$ transients, and the ¹³C HMBC and HSQC with n transients each (where n is some positive integer). This particular ratio yielded the spectra shown in Figure 4; the user may also customise these numbers themselves using the pulse programmes provided in the *Supplementary Information*.

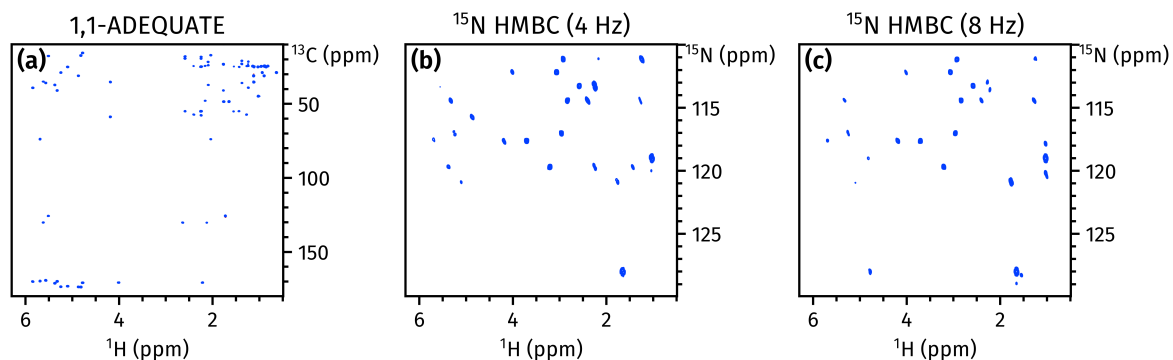


Figure 3: Spectra obtained from the NOAH-3 AB_NB_N supersequence. **(a)** 1,1-ADEQUATE (256 t_1 increments). **(b)** ^{15}N HMBC optimised for $^nJ_{\text{NH}} = 4$ Hz (128 t_1 increments). **(c)** ^{15}N HMBC optimised for $^nJ_{\text{NH}} = 8$ Hz (128 t_1 increments). Spectra were obtained on a 700 MHz Bruker AV III equipped with a TCI H/C/N cryoprobe; the sample used was 50 mM cyclosporin A in C_6D_6 . (Note the ‘wing’ artefacts in the HMBC spectra! I don’t think these are coming from the ADEQUATE, I think it’s more likely to be due to imperfect refocusing by the ^1H 180° pulse. This can be fixed by increasing the CTP gradient duration (compare with Figure 5b where I did this), but that comes with a price—sensitivity drops quite a bit.)

Like the ^{15}N HMBC, the ^{13}C HMBC module simply use up all the $^1\text{H}^{13}\text{C}$ magnetisation preserved by the ADEQUATE. However, the ^{13}C HSQC draws on the same $^1\text{H}^{13}\text{C}$ magnetisation pool. In order to increase the sensitivity of the HSQC experiment, we add a period of isotropic DIPSI-2 mixing²⁹ immediately before the HSQC module to effect $^1\text{H}^{13}\text{C} \rightarrow ^1\text{H}^{13}\text{C}$ magnetisation transfer, as has previously been done in ASAP^{30–33} and NOAH¹⁹ experiments (Figure S2).

The acquisition of the NOAH-4 AB_NBS spectra in Figure 4 took 124 minutes; in contrast, normal acquisition of all four experiments (with the appropriate number of transients) required a total of 223 minutes. As the ADEQUATE is placed first in the supersequence, its sensitivity is almost identical to that of a standalone ADEQUATE; the inclusion of the ZIP element does not have an appreciable impact on this. [Not sure why; we clearly saw at least 10% loss in seHSQC.] The two HMBC spectra experience small losses (16–36%) in sensitivity, due to imperfect magnetisation retention by the ADEQUATE module. This is, however, outweighed by the almost twofold time savings provided by concatenation of the modules: if the NOAH supersequence were acquired for as long as the standalone experiments would, the ^{15}N and ^{13}C HMBC spectra would in fact have –14% and 12% increases in SNR respectively. [The numbers are placeholders for now, reason being that the ABBS expt was acquired with 2.5 ms gradients in ^{15}N HMBC—this leads to a 36% loss compared to the standalone ^{15}N HMBC which was acquired with 1 ms gradients. The ^{13}C HMBC loses 16% which is about right. I don’t think the longer gradients are really necessary, so I’d prefer to redo the experiment to get nicer numbers.] Due to the reuse of $^1\text{H}^{13}\text{C}$ magnetisation, the HSQC module only retains 32% of its original sensitivity. However, as the HSQC is still two orders of magnitude more sensitive than the ADEQUATE, this decrease is readily tolerated; if necessary, the sensitivity-enhanced HSQC module^{19,20,34,35} may also be used in its place.

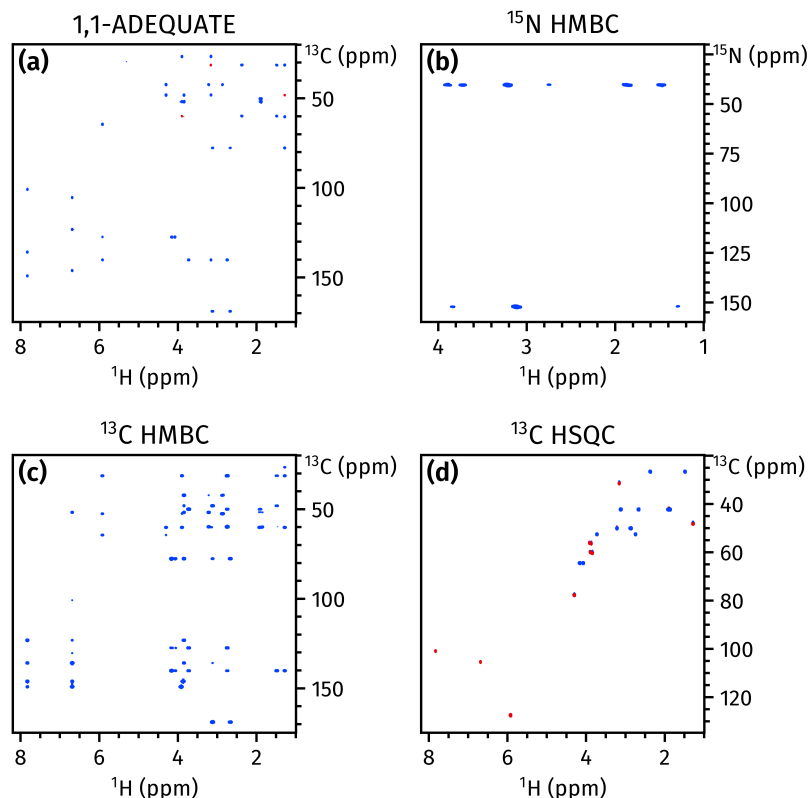


Figure 4: Spectra obtained from the NOAH-4 AB_NBS supersequence. (a) 1,1-ADEQUATE (16 transients). (b) ^{15}N HMBC (12 transients). (c) ^{13}C HMBC (2 transients). (d) ^{13}C HSQC (2 transients). Spectra were obtained on a 700 MHz Bruker AV III equipped with a TCI H/C/N cryoprobe; the sample used was 50 mM brucine in $CDCl_3$.

5 NOAH-5 $AB_NBS_N^+S$

As a final example, we add a further ^{15}N seHSQC module to the above sequence. This is most easily accomplished by simply diverting one ‘thread’ away from the ^{15}N HMBC, meaning that the second slot in the supersequence now alternates between four different experiment (Figure 1e). In principle, the ^{15}N seHSQC uses only $^1H^N$ magnetisation (i.e. protons directly bonded to ^{15}N), and can simply be added as a third module in every ‘thread’ of the supersequence: such an arrangement would maximise its sensitivity as a larger number of transients are collected. However, this would compromise the performance of the *other* modules, as they must then be modified to preserve this magnetisation: for example, the HMBC modules would need to include the *zz*-filter,^{5,6} which generally causes 10–20% sensitivity losses. As the ^{15}N seHSQC is not a particularly demanding experiment in terms of sensitivity, it makes more sense to implement it in this interleaved manner. This example especially illustrates how the use of interleaved *and* sequential acquisition leads to much greater flexibility in supersequence design, especially when considering the relative sensitivities of different modules.

The five spectra thus obtained are shown in Figure 5. Collectively, this supersequence provides virtually all heteronuclear correlation data required for structural elucidation or assignment. This is similar in spirit to

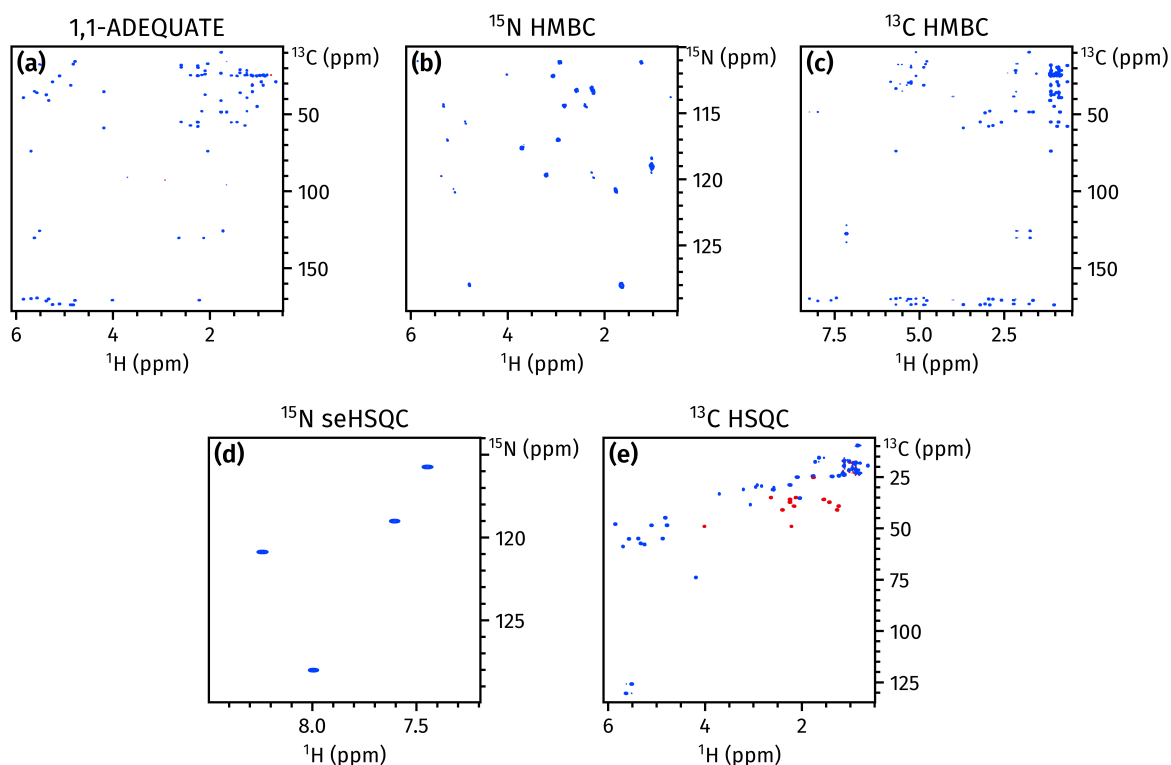


Figure 5: Spectra obtained from the NOAH-5 AB_NBS_N⁺S supersequence. (a) 1,1-ADEQUATE (16 transients). (b) ¹⁵N HMBC (10 transients). (c) ¹³C HMBC (2 transients). (d) ¹⁵N sensitivity-enhanced HSQC (2 transients). (e) ¹³C HSQC (2 transients). Spectra were obtained on a 700 MHz Bruker AV III equipped with a TCI H/C/N cryoprobe; the sample used was 50 mM cyclosporin A in C₆D₆.

the PANACEA experiment,^{36,37} but yields greater sensitivity as it uses equilibrium ¹H magnetisation rather than the low-magnetogyric ratio ¹³C and ¹⁵N nuclei, and does not require multiple-receiver hardware.^{4,38}

It is possible to further combine these spectra using indirect covariance processing^{39–41} to generate other forms of correlation spectra. For example, when processed in this way, the ¹⁵N HMBC and ¹³C HSQC yield ¹³C–¹⁵N correlation spectra.^{42,43} Furthermore, the ¹³C HSQC and ADEQUATE experiments can be used to create ¹³C–¹³C one-bond correlation spectra.^{44,45} It should be further emphasised that all of the ‘base’ spectra used as the inputs here are obtained *in a single measurement* using either the NOAH-4 or NOAH-5 supersequences discussed above.

6 Conclusion(ish)

While the generalised supersequences presented here enable modules to be assembled in almost any imaginable way, their increasing complexity mean that pulse programme construction is more difficult. At present, the GENESIS tool for automatic pulse sequence generation⁴⁶ only provides limited options for parallel supersequences. In particular, it is restricted to only *two* different ‘threads’ (as demonstrated in

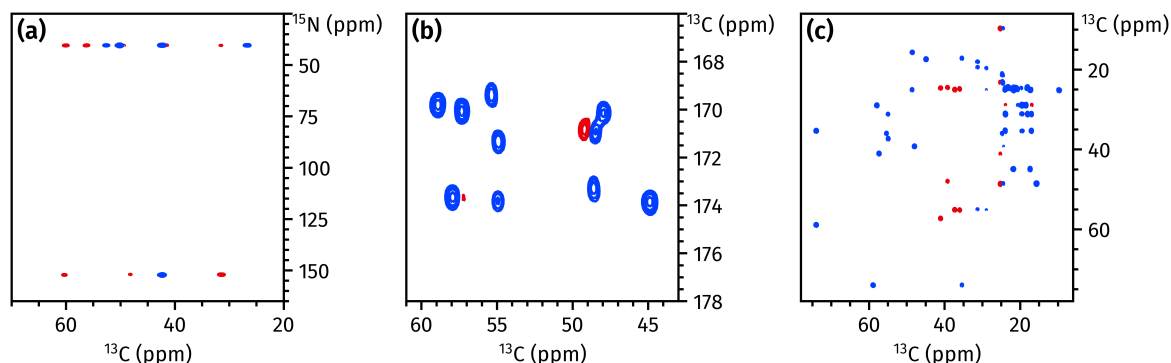


Figure 6: Spectra obtained through indirect covariance processing. (a) ^{13}C – ^{15}N correlation spectrum (containing both one- and multiple-bond correlations) obtained by processing the brucine ^{15}N HMBC and ^{13}C HSQC spectra (in Figures 4b and 4d) using unsymmetric indirect covariance. (b–c) Insets of ^{13}C – ^{13}C one-bond correlation spectrum, obtained by processing the cyclosporin ADEQUATE and ^{13}C HSQC spectra (in Figures 5a and 5e) using generalised indirect covariance ($\lambda = 0.5$). The $\text{C}\alpha$ –CO correlations are shown in (b), and sidechain C–C correlations in (c). (Some of the peaks in (a) and (c) are artefacts. (b) is very satisfying though—11 peaks for 11 residues. I assigned every peak except for those in the top-right corner of (c)... we could crop (c) to show only $\text{C}\alpha$ – $\text{C}\beta$ correlations, which I did completely assign.)

previous work⁷); we hope to expand this in the near future. Different AU programmes are also required to process the data correctly. The pulse sequences and processing scripts used in this work are provided in the Bruker User Library, accessible at <https://www.bruker.com/en/services/bruker-user-library.html>.

In conclusion, we have demonstrated here how low-sensitivity experiments, such as 1,1-ADEQUATE and ^{15}N HMBC, may be combined in NMR supersequences, leading to substantial reductions in experiment time. Using the principles of sequential and interleaved acquisition, further high-sensitivity modules may be added almost at will through a generalisation of our previous concept of ‘parallel’ supersequences, where multiple ‘threads’ are executed and divided between several interleaved modules. The spectra thus obtained provide the chemist with far more powerful tools for the characterisation of complex molecules, especially in cases where existing NOAH supersequences do not provide sufficient information for unambiguous assignment.

Acknowledgements

We thank Dr Mohammadali Foroozandeh (University of Oxford) for helpful discussions. J.R.J.Y. thanks the Clarendon Fund (University of Oxford) and the EPSRC Centre for Doctoral Training in Synthesis for Biology and Medicine (EP/L015838/1) for a studentship, generously supported by AstraZeneca, Diamond Light Source, Defence Science and Technology Laboratory, Evotec, GlaxoSmithKline, Janssen, Novartis, Pfizer, Syngenta, Takeda, UCB, and Vertex.

References

- (1) Findeisen, M.; Berger, S., *50 and More Essential NMR Experiments: A Detailed Guide*; Wiley: Weinheim, 2013.
- (2) Claridge, T. D. W., *High-Resolution NMR Techniques in Organic Chemistry*, 3rd ed.; Elsevier: Amsterdam, 2016.
- (3) Kupče, Ě.; Claridge, T. D. W. NOAH: NMR Supersequences for Small Molecule Analysis and Structure Elucidation. *Angew. Chem., Int. Ed.* **2017**, *56*, 11779–11783, DOI: [10.1002/anie.201705506](https://doi.org/10.1002/anie.201705506).
- (4) Kupče, Ě.; Frydman, L.; Webb, A. G.; Yong, J. R. J.; Claridge, T. D. W. Parallel nuclear magnetic resonance spectroscopy. *Nat. Rev. Methods Primers* **2021**, *1*, 27, DOI: [10.1038/s43586-021-00024-3](https://doi.org/10.1038/s43586-021-00024-3).
- (5) Kupče, Ě.; Claridge, T. D. W. Molecular structure from a single NMR supersequence. *Chem. Commun.* **2018**, *54*, 7139–7142, DOI: [10.1039/c8cc03296c](https://doi.org/10.1039/c8cc03296c).
- (6) Kupče, Ě.; Claridge, T. D. W. New NOAH modules for structure elucidation at natural isotopic abundance. *J. Magn. Reson.* **2019**, *307*, 106568, DOI: [10.1016/j.jmr.2019.106568](https://doi.org/10.1016/j.jmr.2019.106568).
- (7) Kupče, Ě.; Yong, J. R. J.; Widmalm, G.; Claridge, T. D. W. Parallel NMR Supersequences: Ten Spectra in a Single Measurement. *JACS Au* **2021**, DOI: [10.1021/jacsau.1c00423](https://doi.org/10.1021/jacsau.1c00423).
- (8) White, K. N.; Amagata, T.; Oliver, A. G.; Tenney, K.; Wenzel, P. J.; Crews, P. Structure Revision of Spiroleucettadine, a Sponge Alkaloid with a Bicyclic Core Meager in H-Atoms. *J. Org. Chem.* **2008**, *73*, 8719–8722, DOI: [10.1021/jo800960w](https://doi.org/10.1021/jo800960w).
- (9) Senior, M. M.; Williamson, R. T.; Martin, G. E. Using HMBC and ADEQUATE NMR Data To Define and Differentiate Long-Range Coupling Pathways: Is the Crews Rule Obsolete? *J. Nat. Prod.* **2013**, *76*, 2088–2093, DOI: [10.1021/np400562u](https://doi.org/10.1021/np400562u).
- (10) Buevich, A. V.; Williamson, R. T.; Martin, G. E. NMR Structure Elucidation of Small Organic Molecules and Natural Products: Choosing ADEQUATE vs HMBC. *J. Nat. Prod.* **2014**, *77*, 1942–1947, DOI: [10.1021/np500445s](https://doi.org/10.1021/np500445s).
- (11) Crouch, R. C.; Llanos, W.; Mehr, K. G.; Hadden, C. E.; Russell, D. J.; Martin, G. E. Applications of cryogenic NMR probe technology to long-range ^1H – ^{15}N 2D NMR studies at natural abundance. *Magn. Reson. Chem.* **2001**, *39*, 555–558, DOI: [10.1002/mrc.886](https://doi.org/10.1002/mrc.886).
- (12) Martin, G. E.; Williams, A. J. Applications of ^1H – ^{15}N Long-Range Heteronuclear Shift Correlation and ^{15}N NMR in Alkaloid Chemistry. *Annu. Rep. NMR Spectrosc.* **2015**, *84*, 1–76, DOI: [10.1016/b.s.arnmr.2014.10.003](https://doi.org/10.1016/b.s.arnmr.2014.10.003).
- (13) Bax, A.; Freeman, R.; Frenkiel, T. A. An NMR technique for tracing out the carbon skeleton of an organic molecule. *J. Am. Chem. Soc.* **1981**, *103*, 2102–2104, DOI: [10.1021/ja00398a044](https://doi.org/10.1021/ja00398a044).
- (14) Reif, B.; Köck, M.; Kerssebaum, R.; Kang, H.; Fenical, W.; Griesinger, C. ADEQUATE, a New Set of Experiments to Determine the Constitution of Small Molecules at Natural Abundance. *J. Magn. Reson., Ser. A* **1996**, *118*, 282–285, DOI: [10.1006/jmra.1996.0038](https://doi.org/10.1006/jmra.1996.0038).
- (15) Martin, G. E. Using 1,1- and 1,*n*-ADEQUATE 2D NMR Data in Structure Elucidation Protocols. *Annu. Rep. NMR Spectrosc.* **2011**, *74*, 215–291, DOI: [10.1016/B978-0-08-097072-1.00005-4](https://doi.org/10.1016/B978-0-08-097072-1.00005-4).

- (16) Rao Kakita, V. M.; Hosur, R. V. All-in-one NMR spectroscopy of small organic molecules: complete chemical shift assignment from a single NMR experiment. *RSC Adv.* **2020**, *10*, 21174–21179, DOI: [10.1039/d0ra03417g](https://doi.org/10.1039/d0ra03417g).
- (17) Mareci, T. H.; Freeman, R. Echoes and antiechoes in coherence transfer NMR: Determining the signs of double-quantum frequencies. *J. Magn. Reson.* **1982**, *48*, 158–163, DOI: [10.1016/0022-2364\(82\)90250-5](https://doi.org/10.1016/0022-2364(82)90250-5).
- (18) Orts, J.; Gossert, A. D. Structure determination of protein-ligand complexes by NMR in solution. *Methods* **2018**, *138–139*, 3–25, DOI: [10.1016/j.ymeth.2018.01.019](https://doi.org/10.1016/j.ymeth.2018.01.019).
- (19) Yong, J. R. J.; Hansen, A. L.; Kupče, Ě.; Claridge, T. D. W. Increasing sensitivity and versatility in NMR supersequences with new HSQC-based modules. *J. Magn. Reson.* **2021**, *329*, 107027, DOI: [10.1016/j.jmr.2021.107027](https://doi.org/10.1016/j.jmr.2021.107027).
- (20) Hansen, A. L.; Kupče, Ě.; Li, D.-W.; Bruschweiler-Li, L.; Wang, C.; Brüschweiler, R. 2D NMR-Based Metabolomics with HSQC/TOCSY NOAH Supersequences. *Anal. Chem.* **2021**, *93*, 6112–6119, DOI: [10.1021/acs.analchem.0c05205](https://doi.org/10.1021/acs.analchem.0c05205).
- (21) Sørensen, O. W. Selective Rotations Using Non-Selective Pulses and Heteronuclear Couplings. *Bull. Magn. Reson.* **1994**, *16*, 49–53.
- (22) Nagy, T. M.; Gyöngyösi, T.; Kövér, K. E.; Sørensen, O. W. BANGO SEA XLOC/HMBC–H2OBC: complete heteronuclear correlation within minutes from one NMR pulse sequence. *Chem. Commun.* **2019**, *55*, 12208–12211, DOI: [10.1039/c9cc06253j](https://doi.org/10.1039/c9cc06253j).
- (23) Nagy, T. M.; Kövér, K. E.; Sørensen, O. W. NORD: NO Relaxation Delay NMR Spectroscopy. *Angew. Chem., Int. Ed.* **2021**, *60*, 13587–13590, DOI: [10.1002/anie.202102487](https://doi.org/10.1002/anie.202102487).
- (24) Wagner, R.; Berger, S. ACCORD-HMBC: a superior technique for structural elucidation. *Magn. Reson. Chem.* **1998**, *36*, S44–S46, DOI: [10.1002/\(sici\)1097-458x\(199806\)36:13<s44::aid-omr281>3.0.co;2-q](https://doi.org/10.1002/(sici)1097-458x(199806)36:13<s44::aid-omr281>3.0.co;2-q).
- (25) Martin, G. E.; Hadden, C. E.; Crouch, R. C.; Krishnamurthy, V. V. ACCORD-HMBC: advantages and disadvantages of static versus accordion excitation. *Magn. Reson. Chem.* **1999**, *37*, 517–528, DOI: [10.1002/\(sici\)1097-458x\(199908\)37:8<517::aid-mrc501>3.0.co;2-w](https://doi.org/10.1002/(sici)1097-458x(199908)37:8<517::aid-mrc501>3.0.co;2-w).
- (26) Hadden, C. E.; Martin, G. E.; Krishnamurthy, V. V. Improved Performance Accordion Heteronuclear Multiple-Bond Correlation Spectroscopy—IMPEACH-MBC. *J. Magn. Reson.* **1999**, *140*, 274–280, DOI: [10.1006/jmre.1999.1840](https://doi.org/10.1006/jmre.1999.1840).
- (27) Martin, G. E.; Hadden, C. E. Application of accordion excitation in ^1H – ^{15}N long-range heteronuclear shift correlation experiments at natural abundance. *Magn. Reson. Chem.* **2000**, *38*, 251–256, DOI: [10.1002/\(sici\)1097-458x\(200004\)38:4<251::aid-mrc625>3.0.co;2-j](https://doi.org/10.1002/(sici)1097-458x(200004)38:4<251::aid-mrc625>3.0.co;2-j).
- (28) Hadden, C. E.; Martin, G. E.; Krishnamurthy, V. V. Constant time inverse-detection gradient accordion rescaled heteronuclear multiple bond correlation spectroscopy: CIGAR-HMBC. *Magn. Reson. Chem.* **2000**, *38*, 143–147, DOI: [10.1002/\(sici\)1097-458x\(200002\)38:2<143::aid-mrc624>3.0.co;2-s](https://doi.org/10.1002/(sici)1097-458x(200002)38:2<143::aid-mrc624>3.0.co;2-s).
- (29) Shaka, A. J.; Lee, C. J.; Pines, A. Iterative schemes for bilinear operators; application to spin decoupling. *J. Magn. Reson.* **1988**, *77*, 274–293, DOI: [10.1016/0022-2364\(88\)90178-3](https://doi.org/10.1016/0022-2364(88)90178-3).

- (30) Schulze-Sünninghausen, D.; Becker, J.; Luy, B. Rapid Heteronuclear Single Quantum Correlation NMR Spectra at Natural Abundance. *J. Am. Chem. Soc.* **2014**, *136*, 1242–1245, DOI: [10.1021/ja411588d](https://doi.org/10.1021/ja411588d).
- (31) Schulze-Sünninghausen, D.; Becker, J.; Koos, M. R. M.; Luy, B. Improvements, extensions, and practical aspects of rapid ASAP-HSQC and ALSOFAST-HSQC pulse sequences for studying small molecules at natural abundance. *J. Magn. Reson.* **2017**, *281*, 151–161, DOI: [10.1016/j.jmr.2017.05.012](https://doi.org/10.1016/j.jmr.2017.05.012).
- (32) Koos, M. R. M.; Luy, B. Polarization recovery during ASAP and SOFAST/ALSOFAST-type experiments. *J. Magn. Reson.* **2019**, *300*, 61–75, DOI: [10.1016/j.jmr.2018.12.014](https://doi.org/10.1016/j.jmr.2018.12.014).
- (33) Becker, J.; Koos, M. R. M.; Schulze-Sünninghausen, D.; Luy, B. ASAP-HSQC-TOCSY for fast spin system identification and extraction of long-range couplings. *J. Magn. Reson.* **2019**, *300*, 76–83, DOI: [10.1016/j.jmr.2018.12.021](https://doi.org/10.1016/j.jmr.2018.12.021).
- (34) Palmer, A. G.; Cavanagh, J.; Wright, P. E.; Rance, M. Sensitivity improvement in proton-detected two-dimensional heteronuclear correlation NMR spectroscopy. *J. Magn. Reson.* **1991**, *93*, 151–170, DOI: [10.1016/0022-2364\(91\)90036-S](https://doi.org/10.1016/0022-2364(91)90036-S).
- (35) Kay, L.; Keifer, P.; Saarinen, T. Pure absorption gradient enhanced heteronuclear single quantum correlation spectroscopy with improved sensitivity. *J. Am. Chem. Soc.* **1992**, *114*, 10663–10665, DOI: [10.1021/ja00052a088](https://doi.org/10.1021/ja00052a088).
- (36) Kupče, Ě.; Freeman, R. Molecular Structure from a Single NMR Experiment. *J. Am. Chem. Soc.* **2008**, *130*, 10788–10792, DOI: [10.1021/ja8036492](https://doi.org/10.1021/ja8036492).
- (37) Kupče, Ě.; Freeman, R. Molecular structure from a single NMR sequence (fast-PANACEA). *J. Magn. Reson.* **2010**, *206*, 147–153, DOI: [10.1016/j.jmr.2010.06.018](https://doi.org/10.1016/j.jmr.2010.06.018).
- (38) Kupče, Ě.; Mote, K. R.; Webb, A.; Madhu, P. K.; Claridge, T. D. W. Multiplexing experiments in NMR and multi-nuclear MRI. *Prog. Nucl. Magn. Reson. Spectrosc.* **2021**, *124-125*, 1–56, DOI: [10.1016/j.pnmrs.2021.03.001](https://doi.org/10.1016/j.pnmrs.2021.03.001).
- (39) Zhang, F.; Brüschweiler, R. Indirect Covariance NMR Spectroscopy. *J. Am. Chem. Soc.* **2004**, *126*, 13180–13181, DOI: [10.1021/ja047241h](https://doi.org/10.1021/ja047241h).
- (40) Snyder, D. A.; Brüschweiler, R. Generalized Indirect Covariance NMR Formalism for Establishment of Multidimensional Spin Correlations. *J. Phys. Chem. A* **2009**, *113*, 12898–12903, DOI: [10.1021/jp9070168](https://doi.org/10.1021/jp9070168).
- (41) Jaeger, M.; Aspers, R. L. E. G. Covariance NMR and Small Molecule Applications. *Annu. Rep. NMR Spectrosc.* **2014**, *83*, 271–349, DOI: [10.1016/B978-0-12-800183-7.00005-8](https://doi.org/10.1016/B978-0-12-800183-7.00005-8).
- (42) Martin, G. E.; Hilton, B. D.; Irish, P. A.; Blinov, K. A.; Williams, A. J. ^{13}C – ^{15}N connectivity networks via unsymmetrical indirect covariance processing of ^1H – ^{13}C HSQC and ^1H – ^{15}N IMPEACH spectra. *Journal of Heterocyclic Chemistry* **2007**, *44*, 1219–1222, DOI: [10.1002/jhet.5570440541](https://doi.org/10.1002/jhet.5570440541).
- (43) Martin, G. E.; Irish, P. A.; Hilton, B. D.; Blinov, K. A.; Williams, A. J. Utilizing unsymmetrical indirect covariance processing to define ^{15}N – ^{13}C connectivity networks. *Magn. Reson. Chem.* **2007**, *45*, 624–627, DOI: [10.1002/mrc.2029](https://doi.org/10.1002/mrc.2029).

- (44) Martin, G. E.; Hilton, B. D.; Blinov, K. A. HSQC-ADEQUATE correlation: a new paradigm for establishing a molecular skeleton. *Magn. Reson. Chem.* **2011**, *49*, 248–252, DOI: [10.1002/mrc.2743](https://doi.org/10.1002/mrc.2743).
- (45) Martin, G. E.; Hilton, B. D.; Willcott III, M. R.; Blinov, K. A. HSQC-ADEQUATE: an investigation of data requirements. *Magn. Reson. Chem.* **2011**, *49*, 350–357, DOI: [10.1002/mrc.2757](https://doi.org/10.1002/mrc.2757).
- (46) Yong, J. R. J.; Kupče, Ě.; Claridge, T. D. W. Modular Pulse Program Generation for NMR Supersequences. *Anal. Chem.* **2022**, *94*, 2271–2278, DOI: [10.1021/acs.analchem.1c04964](https://doi.org/10.1021/acs.analchem.1c04964).

Supporting Information

for

Uniting Low- and High-Sensitivity
Experiments through Generalised NMR
Supersequences

Jonathan R. J. Yong,¹ Ēriks Kupče,² Tim D. W. Claridge^{1,*}

¹ *Chemistry Research Laboratory, Department of Chemistry, University of Oxford,
Mansfield Road, Oxford, OX1 3TA, United Kingdom*

² *Bruker UK Ltd, R&D, Coventry CV4 9GH, United Kingdom*

* tim.claridge@chem.ox.ac.uk

Contents

S1 Pulse programme setup	S2
S2 Spectra that didn't make it into the main text	S2
S3 ABBS comparison with and without DIPSI	S3

S1 Pulse programme setup

For ABBS, the thought process is generally as follows:

- Decide on number of t_1 increments for each module (we call this N_1). This is determined by desired resolution in indirect dimension. Say 256.
- Decide on NS for each module. NS for ADEQUATE must be equal to sum of NS for all other modules.
- Determine the gcd of the separate NS's (for example, $\text{gcd}(16, 12, 2, 2) = 2$). Set the TopSpin parameter NS as this value. Make sure this is at least 2 as this determines the minimum phase cycle
- Set (cnst51, cnst52, cnst53, cnst54) = NS's divided through by their gcd (so 8, 6, 1, 1). In practice the last of these is automatically calculated, so it doesn't have to be set.
- Set NBL = 2 since there are only really two 'horizontally' combined modules.
- Set TopSpin TD1 parameter to be $N_1 \times \text{NBL} \times \text{cnst51}$. In this case, $256 \times 2 \times 8 = 4096$.

Should note here that previous parallel supersequences¹ essentially follow the same idea but with two threads. The sequences don't explicitly use the cnst parameters as shown above, but in practice they behave exactly as if $\text{cnst51} = 2$ and $\text{cnst52} = \text{cnst53} = 1$.

This observation, in principle, should open up a 'path' to generalising the GENESIS algorithm—but I need time to do it. Providing a GUI is also problematic. (I have some *ideas* about the desired UI, but actually *implementing* it is another matter...)

S2 Spectra that didn't make it into the main text

(We should move some figures from the main text to here—the only question is which ones?)

Since the ^1H - ^1H NOESY uses the same $^1\text{H}^1\text{C}$ magnetisation as ^{13}C HMBC so can be directly substituted in its place, leading to a NOAH-4 AB_NNS supersequence (Figure S1). This not only provides a wealth of through-bond correlations which aid in elucidating molecular constitution, but also furnishes through-space correlations for the determination of configuration or conformation.

One *actual* problem here is the receiver gain. For ABBS I had $\text{RG} = 2050$, but for this I had to set $\text{RG} = 29(!!)$.

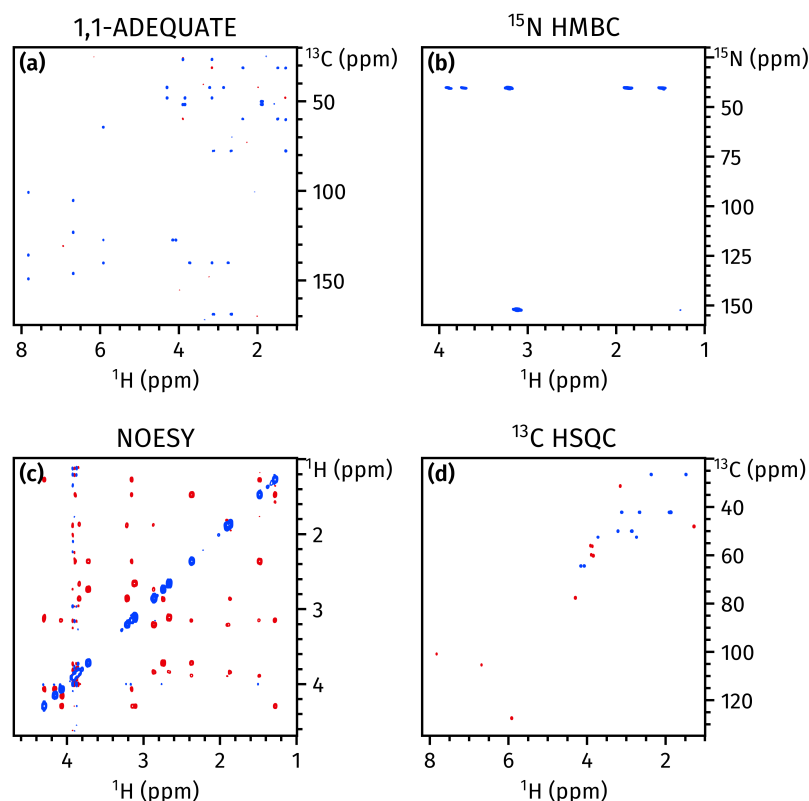


Figure S1: Spectra obtained from the NOAH-4 AB_NNS supersequence. **(a)** 1,1-ADEQUATE (16 transients). **(b)** ¹⁵N HMBC (12 transients). **(c)** NOESY (2 transients, 800 ms mixing time). **(d)** ¹³C HSQC (2 transients). Spectra were obtained on a 700 MHz Bruker AV III equipped with a TCI H/C/N cryoprobe; the sample used was 50 mM brucine in CDCl₃.

S3 ABBS comparison with and without DIPSI

The average signal enhancement across all peaks is 88% (Figure S2).

Similar to results seen previously²

References

- (1) Kupče, Ě.; Yong, J. R. J.; Widmalm, G.; Claridge, T. D. W. Parallel NMR Supersequences: Ten Spectra in a Single Measurement. *JACS Au* **2021**, DOI: [10.1021/jacsau.1c00423](https://doi.org/10.1021/jacsau.1c00423).
- (2) Yong, J. R. J.; Hansen, A. L.; Kupče, Ě.; Claridge, T. D. W. Increasing sensitivity and versatility in NMR supersequences with new HSQC-based modules. *J. Magn. Reson.* **2021**, 329, 107027, DOI: [10.1016/j.jmr.2021.107027](https://doi.org/10.1016/j.jmr.2021.107027).

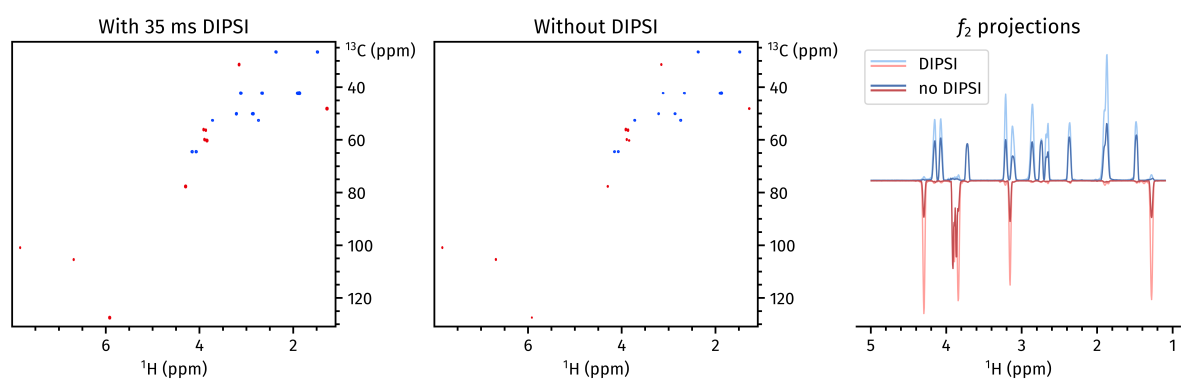


Figure S2: ^{13}C HSQC spectra obtained from the NOAH-4 AB_N BS experiment (Figure 1d). **(a)** Without DIPSI mixing between the ADEQUATE and ^{13}C HSQC modules. **(b)** With 35 ms DIPSI mixing between the ADEQUATE and ^{13}C HSQC modules (this spectrum is the same as in Figure 4d). **(c)** Projections of the spectra in **(a)** and **(b)** onto the f_2 axis. Spectra were obtained on a 700 MHz Bruker AV III equipped with a TCI H/C/N cryoprobe; the sample used was 50 mM brucine in CDCl_3 .